Journal of Mathematical Extension
Vol. 17, No. 9, (2023) (3)1-28
URL: https://doi.org/10.30495/JME.2023.2775
ISSN: 1735-8299
Original Research Paper

Chemostat Model Analysis Using Various Kernels with Fractional Derivatives

A. Akgül*
Siirt University
Saveetha School of Engineering, SIMATS

E. Ülgül
Siirt University

R.T. Alqahtani
Imam Mohammad Ibn Saud Islamic University

Abstract. The investigation involves utilizing a set of three ordinary differential equations to mathematically model the degradation process of a mixture containing phenol and p-cresol within a continuously agitated bioreactor. The primary focus lies in the stability analysis of equilibrium points within this model. Additionally, the research delves into exploring the influence of fractal dimension and fractional order on the model, incorporating fractal-fractional derivatives and employing three distinct types of kernels.

To quantify the concentrations of phenol, p-cresol, and biomass, highly effective computational algorithms have been formulated, enhancing the precision and efficiency of data analysis. In conclusion, the proposed methodology's soundness and accuracy are thoroughly scrutinized and affirmed through extensive computational simulations.

Keywords and Phrases: Bioreactor Model, Computational Methods, Fractal-Fractional Derivatives, Computational Simulations.

Received: June 2023; Accepted: October 2023
*Corresponding Author

1 Introduction

There are numerous scientific articles that describe the discovery and work of microbial species that have greater chemical compound degradation activity [7]. Numerous individual microorganisms have been studied in [24]. The nature of the particular mixture and the used microbes determine whether one or all chemical components will biodegrade [25, 27, 28, 17]. The classical derivatives have a significant extension in fractional calculus. Fractional differential equations (FDEs) have recently been used in a variety of disciplines. Many authors have worked on these equations such as KdV equation [22], advection-dispersion equation [18], telegraph equation [14], Schrodinger equation [3], heat equation [16], convection diffusion equation [6], Fokker Planck equation [19]. Some of the FDEs do not have exact solution, therefore it is required to work on computational methods to solve the mentioned equations such as solving nonlinear fractional diffusion wave equation with homotopy analysis technique [23], solving PDEs of fractal order by Adomian decomposition method [8]. Boutiara A. at el.[4] examines the first order (p, q)-difference boundary conditions for the fractional (p, q)-difference equation's current solution in generalized metric space. We use the numerical methods of the Lipschitz matrix and vector norms in conjunction with some contraction techniques from fixed point theory to arrive at the solution. George R. at el. [11] considered the Hilfer type fractional operator to examine the proposed integral equation. The capabilities of measurement theory and fixed point techniques were used to provide the necessary space to guarantee the existence of the solution. George R. at el. [13] investigated the existence of a solution to the fractional pantograph equation using a new method. George R. at el.[12] aimed to establish conditions for the existence, uniqueness and Ulam-Hyers stability of solutions for a coupled pantograph problem system with three consecutive fractional derivatives. In [7], the authors have given a bioreactor model but they do not consider the death rate of bacteria and also general configuration of the reactor. We have provided the bioreactor model with the fractal-fractional derivatives (FFD). The model with fractal-fractional derivatives has never been analysed so far. Our model includes the death rate of bacteria which is important in environment of the process. We also consider general configuration of the reactor where

our model includes a membrane and continuous reactor. Additionally, we fractionalize the model and apply a novel computational technique to get the computational simulations. We organize our manuscript as follow. Problem formulation is done in Section 2. In Section 3 we have discussed the analysis of the model in the classical case and presented the equilibria and stability analysis. Sections 4, 5 and 6 deals with analysis of the model with three different kernels viz the power-law kernel, the exponential-decay kernel and the Mittag-Leffler kernel respectively and in section 7 we demonstrate the computational simulations.

2 Preliminaries

The following definitions of FFD and fractal-fractional integral (FFI) with three different kernels are taken from [1] .

Definition 2.1. The FFD with power-law type kernel is described as:

$$ {}_{c}^{FFP}D_{t}^{\alpha,\eta} f(t) = \frac{1}{1-\alpha}\frac{d}{du^{\eta}}\int_{c}^{t} f(s)(t-s)^{-\alpha}ds,\ 0<\alpha,\eta\leq 1, \tag{1} $$

where,

$$ \frac{df(s)}{ds^{\eta}} = \lim_{t\to s}\frac{f(t)-f(s)}{t^{\eta}-s^{\eta}} \tag{2} $$

Definition 2.2. The FFD with exponential-decay type kernel is described as:

$$ {}_{c}^{FFE}D_{t}^{\alpha,\eta} f(t) = \frac{M_1(\alpha)}{1-\alpha}\frac{d}{dt^{\eta}}\int_{c}^{t} f(s)\exp\Big(\frac{-\alpha}{1-\alpha}(t-s)\Big)ds,\ 0<\alpha,\eta\leq 1. \tag{3} $$

Definition 2.3. The FFD with Mittag-Leffler type kernel is described as:

$$ {}_{c}^{FFM}D_{t}^{\alpha,\eta} f(t) = \frac{AB(\alpha)}{1-\alpha}\frac{d}{dt^{\eta}}\int_{c}^{t} f(s)E_{\alpha}\Big(\frac{-\alpha}{1-\alpha}(t-s)^{\alpha}\Big)ds,\ 0<\alpha,\eta\leq 1, \tag{4} $$

where, $AB(\alpha) = 1-\alpha+\frac{\alpha}{\Gamma(\alpha)}$.

Definition 2.4. The FFI with power-law type kernel is described as:

$$ {}_0^{FFP}I_t^{\alpha,\eta} f(t) = \frac{\eta}{\Gamma(\alpha)} \int_0^t (t-s)^{\alpha-1} s^{\tau-1} \phi(s) ds. \tag{5} $$

Definition 2.5. The FFI with exponential-decay type kernel is described as:

$$ {}_0^{FFE}I_t^{\alpha,\eta} f(t) = \frac{\alpha\eta}{M_1(\alpha)} \int_0^t s^{\alpha-1} f(s) ds + \frac{\tau(1-\alpha)t^{\tau-1}}{M_1(\alpha)} \phi(t). \tag{6} $$

Definition 2.6. The FFI with Mittag-Leffler type kernel is described as:

$$ {}_0^{FFM}I_t^{\alpha,\eta} f(t) = \frac{\alpha\eta}{AB(\alpha)} \int_0^t s^{\alpha-1} f(s)(t-s)^{\alpha-1} ds + \frac{\tau(1-\alpha)t^{\tau-1}}{AB(\alpha)} f(t). \tag{7} $$

3 Formation of the Model

Here, we provide the model that will be examined in this study. The three-dimensional model is provided as follows:

$$ \frac{\mathrm{d}S_{ph}}{\mathrm{d}t} = D\left(S_{ph0} - S_{ph}\right) - k_{ph} \cdot \mu\left(S_{ph}, S_{cr}\right) \cdot X, \tag{8} $$

$$ \frac{\mathrm{d}S_{cr}}{\mathrm{d}t} = D\left(S_{cr0} - S_{cr}\right) - k_{cr} \cdot \mu\left(S_{ph}, S_{cr}\right) \cdot X, \tag{9} $$

$$ \frac{\mathrm{d}X}{\mathrm{d}t} = -D\beta X + \mu\left(S_{ph}, S_{cr}\right) X, \tag{10} $$

$$ \mu\left(S_{ph}, S_{cr}\right) = \frac{\mu_{max(ph)} S_{ph}}{K_{s(ph)} + S_{ph} + \frac{S_{ph}^2}{k_{i(ph)}} + I_{cr/ph} S_{cr}} + \frac{\mu_{max(cr)} S_{cr}}{K_{s(cr)} + S_{cr} + \frac{S_{cr}^2}{k_{i(cr)}} + I_{ph/cr} S_{ph}}, \tag{11} $$

The model parameters and variables are detailed in [7]. The parameter β is presented in the general configuration. When $\beta = 1$ we have continued the reactor. When $\beta = 0$ we have a membrane reactor.

4 Analysis of the Model in Classical Sense

We will now start by performing a traditional analysis of the model's attributes.

4.1 Equilibria and Stability Analysis

We take into account how many model (8- 10) equilibrium solutions there are. The model clearly has a branch of the washout specified by:

$$E_0 = (S_{ph}, S_{cr}, X) = (S_{ph0}, S_{cr0}, 0)\,. \tag{12}$$

We obtain the steady state solution of (8- 10) by setting to zero the right side. From the model (8- 10), we have,

$$\begin{aligned} S_{cr} &= \frac{S_{cr0}k_{ph} + k_{cr}(S_{ph} - S_{ph0})}{k_{ph}}, \\ X &= \frac{D\,(S_{ph0} - S_{ph})}{k_{ph}\ (\beta\, D)}. \end{aligned} \tag{13}$$

$$f = \begin{pmatrix} -k_{cr}\mu(s_{ph},s_{cr})X \\ \mu(s_{ph},s_{cr})X \end{pmatrix}$$

$$F = \begin{bmatrix} \frac{\partial\mu(s_{ph},s_{cr})(-k_{cr})X}{\partial(s_{ph},s_{cr})X} & -k_{cr}\mu(s_{ph},s_{cr}) \\ \\ \frac{\partial\mu(s_{ph},s_{cr})X}{\partial(s_{ph},s_{cr})X} & \mu(s_{ph},s_{cr})k_{cr}(s_{ph},s_{cr}) \end{bmatrix}$$

$$V = \begin{pmatrix} -D(s_{cr0}-s_{cr}) \\ D\beta X \end{pmatrix} \quad \rightarrow \quad V = \begin{bmatrix} D & 0 \\ \\ 0 & D\beta \end{bmatrix} \ , V^{-1} = \begin{bmatrix} D\beta & 0 \\ \\ 0 & D \end{bmatrix}$$

$$FV^{-1} = \begin{bmatrix} 0 & -k_{cr}\mu(s_{ph},s_{cr}) \\ \\ 0 & \mu(s_{ph},s_{cr}) \end{bmatrix} \begin{bmatrix} D & 0 \\ \\ 0 & D\beta \end{bmatrix} = \begin{bmatrix} 0 & -Dk_{cr}\mu(s_{ph},s_{cr}) \\ \\ 0 & D\mu(s_{ph},s_{cr}) \end{bmatrix}$$

$$det\left[\ FV^{-1} - \lambda I_2\ \right] = 0 \quad , \begin{vmatrix} -\lambda & -Dk_{cr}\mu(s_{ph},s_{cr}) \\ \\ 0 & D\mu(s_{ph},s_{cr}) - \lambda \end{vmatrix} = 0$$

Thus, we obtain $\lambda_1 = 0, \quad \lambda_2 = D\mu(s_{ph}, s_{cr}) = R_0$

Lemma 4.1. *The steady state solution E_0 is locally asymptotically stable when $D > D_{cr}$ and is unstable when $D < D_{cr}$.*

Proof. We have

$$E_0 = (s_{ph}, s_{cr}, x) = (s_{ph0}, s_{cr0}, 0)$$

$$J(E_0) = \begin{bmatrix} -D - \frac{\partial \mu(s_{ph},s_{cr})}{\partial s_{ph}} k_{ph} x & -\frac{\partial \mu(s_{ph},s_{cr})}{\partial s_{ph}} k_{ph} x & -\mu(s_{ph}, s_{cr}) k_{ph} \\ -k_{cr} \frac{\partial \mu(s_{ph},s_{cr})}{\partial s_{ph}} x & -D - \frac{\partial \mu(s_{ph},s_{cr})}{\partial s_{ph}} k_{cr} x & -\mu(s_{ph}, s_{cr}) k_{cr} \\ \frac{\partial \mu(s_{ph},s_{cr})}{\partial s_{ph}} x & -\frac{\partial \mu(s_{ph},s_{cr})}{\partial s_{ph}} x & -D\beta + \mu(s_{ph}, s_{cr}) \end{bmatrix}$$

$$J(E_0) = \begin{bmatrix} -D & 0 & -\mu(s_{ph0}, s_{cr0}) k_{ph} \\ 0 & -D & -\mu(s_{ph0}, s_{cr0}) k_{cr} \\ 0 & 0 & -D\beta + \mu(s_{ph0}, s_{cr0}) \end{bmatrix}$$

where

$$\mu(s_{ph}, s_{cr}) = \frac{\mu_{max(ph)} s_{ph}}{K_{s(ph)} + s_{ph} + \frac{s_{ph}^2}{K_{i(ph)}} + I_{cr/ph} s_{cr}} + \frac{\mu_{max(cr)} s_{ph}}{K_{s(cr)} + s_{cr} + \frac{s_{cr}^2}{K_{i(cr)}} + I_{ph/cr} s_{ph}}$$

$$\det[J(E_0) - \lambda I_3] = \begin{vmatrix} -D - \lambda & 0 & -\mu(s_{ph}, s_{cr}) k_{ph} \\ 0 & -D - \lambda & -\mu(s_{ph}, s_{cr}) k_{cr} \\ 0 & 0 & \mu(s_{ph}, s_{cr}) - D\beta - \lambda \end{vmatrix} = 0$$

$$= (-D - \lambda)(-D - \lambda)(\mu(s_{ph}, s_{cr}) - D\beta - \lambda) = 0$$

$$\lambda_1 = -D, \quad \lambda_2 = -D, \quad \lambda_3 = -\beta D + \mu(s_{ph}, s_{cr})$$

and

$$\mu(s_{ph}, s_{cr}) = {}^{-} \, max_{ph} s_{ph0} (k_{sph} + s_{ph0} + \frac{s_{ph0}^2}{K_{i(ph)}} + I_{cr/ph} s_{cr0})^{-1} + {}^{-} \, max_{cr} s_{cr0} (k_{scr} + s_{cr0} + \frac{s_{cr0}^2}{K_{i(ph)}} + I_{ph/cr} s_{ph0})^{-1}$$

$$D_{cr} = \frac{k_{icr} k_{ph} (s_{cr0} k_{ph} - s_{ph0} k_{cr})^{-} max_{cr}}{[k_{icr} k_{ph} (K_{scr} k_{ph} + s_{cr0} k_{ph} - s_{ph0} k_{cr}) + (s_{cr} k_{ph} - s_{ph0} k_{cr})^2] \, \beta}$$

If $D > D_{cr}$, then $\lambda_3 < 0$. Thus, all eigenvalues are negative. This presents that the steady state solution E_0 is locally asymptotically stable. $\square$

5 Analysis of the Model with the Power-law Kernel

Here we analyze the model with FFD using the power-law kernel as:

$$
\begin{aligned}
{}_0^{FFP}D_t^{\alpha,\eta}S_{ph} &= D\left(S_{ph0} - S_{ph}\right) - k_{ph}\cdot\mu\left(S_{ph}, S_{cr}\right)\cdot X, && (14)\\
{}_0^{FFP}D_t^{\alpha,\eta}S_{cr} &= D\left(S_{cr0} - S_{cr}\right) - k_{cr}\cdot\mu\left(S_{ph}, S_{cr}\right)\cdot X, && (15)\\
{}_0^{FFP}D_t^{\alpha,\eta}X &= -D\beta X + \mu\left(S_{ph}, S_{cr}\right)X && (16)
\end{aligned}
$$

We have [1]:

$$D^{\eta}f(t) = \frac{f'(t)}{\eta t^{\eta-1}}. \tag{17}$$

Then, we acquire

$$
\begin{aligned}
{}_0^{RL}D_t^{\alpha}S_{ph} &= \eta t^{\eta-1}\left(D\left(S_{ph0} - S_{ph}\right) - k_{ph}\cdot\mu\left(S_{ph}, S_{cr}\right)\cdot X\right), && (18)\\
{}_0^{RL}D_t^{\alpha}S_{cr} &= \eta t^{\eta-1}\left(D\left(S_{cr0} - S_{cr}\right) - k_{cr}\cdot\mu\left(S_{ph}, S_{cr}\right)\cdot X\right), && (19)\\
{}_0^{RL}D_t^{\alpha}X &= \eta t^{\eta-1}\left(-D\beta X + \mu\left(S_{ph}, S_{cr}\right)X\right) && (20)
\end{aligned}
$$

For simplicity, we define

$$
\begin{aligned}
A(t, S_{ph}, S_{cr}, X) &= \eta t^{\eta-1}\left(D\left(S_{ph0} - S_{ph}\right) - k_{ph}\cdot\mu\left(S_{ph}, S_{cr}\right)\cdot X\right), && (21)\\
B(t, S_{ph}, S_{cr}, X) &= \eta t^{\eta-1}\left(D\left(S_{cr0} - S_{cr}\right) - k_{cr}\cdot\mu\left(S_{ph}, S_{cr}\right)\cdot X\right), && (22)\\
C(t, S_{ph}, S_{cr}, X) &= \eta t^{\eta-1}\left(-D\beta X + \mu\left(S_{ph}, S_{cr}\right)X\right) && (23)
\end{aligned}
$$

Then, we obtain

$$
\begin{aligned}
{}_0^{RL}D_t^{\alpha}S_{ph} &= A(t, S_{ph}, S_{cr}, X) && (24)\\
{}_0^{RL}D_t^{\alpha}S_{cr} &= B(t, S_{ph}, S_{cr}, X) && (25)\\
{}_0^{RL}D_t^{\alpha}X &= C(t, S_{ph}, S_{cr}, X) && (26)
\end{aligned}
$$

Applying the Riemann-Liouville integral yields:

$$S_{ph}(t) - S_{ph}(0) = \frac{1}{\Gamma(\alpha)} \int_0^t A(\tau, S_{ph}, S_{cr}, X)(t-\tau)^{\alpha-1} d\tau \tag{27}$$

$$S_{cr}(t) - S_{cr}(0) = \frac{1}{\Gamma(\alpha)} \int_0^t B(\tau, S_{ph}, S_{cr}, X)(t-\tau)^{\alpha-1} d\tau \tag{28}$$

$$X(t) - X(0) = \frac{1}{\Gamma(\alpha)} \int_0^t C(\tau, S_{ph}, S_{cr}, X)(t-\tau)^{\alpha-1} d\tau \tag{29}$$

Discretizing the above equations at t_{n+1}, we get:

$$S_{ph}(t_{n+1}) - S_{ph}(0) = \frac{1}{\Gamma(\alpha)} \int_0^{t_{n+1}} A(\tau, S_{ph}, S_{cr}, X)(t_{n+1}-\tau)^{\alpha-1} d\tau \tag{30}$$

$$S_{cr}(t_{n+1}) - S_{cr}(0) = \frac{1}{\Gamma(\alpha)} \int_0^{t_{n+1}} B(\tau, S_{ph}, S_{cr}, X)(t_{n+1}-\tau)^{\alpha-1} d\tau \tag{31}$$

$$X(t_{n+1}) - X(0) = \frac{1}{\Gamma(\alpha)} \int_0^{t_{n+1}} C(\tau, S_{ph}, S_{cr}, X)(t_{n+1}-\tau)^{\alpha-1} d\tau \tag{32}$$

$$S_{ph}(t_{n+1}) - S_{ph}(0) = \frac{1}{\Gamma(\alpha)} \sum_{j=0}^{n} \int_{t_j}^{t_{j+1}} A(\tau, S_{ph}, S_{cr}, X)(t_{n+1}-\tau)^{\alpha-1} d\tau \tag{33}$$

$$S_{cr}(t_{n+1}) - S_{cr}(0) = \frac{1}{\Gamma(\alpha)} \sum_{j=0}^{n} \int_{t_j}^{t_{j+1}} B(\tau, S_{ph}, S_{cr}, X)(t_{n+1}-\tau)^{\alpha-1} d\tau \tag{34}$$

$$X(t_{n+1}) - X(0) = \frac{1}{\Gamma(\alpha)} \sum_{j=0}^{n} \int_{t_j}^{t_{j+1}} C(\tau, S_{ph}, S_{cr}, X)(t_{n+1}-\tau)^{\alpha-1} d\tau \tag{35}$$

Two-step Lagrange polynomial is used as:

$$p_j(\tau, S_{ph}, S_{cr}, X) = \frac{\tau - t_{j-1}}{t_j - t_{j-1}} A(t_j, S_{ph}, S_{cr}, X) \tag{36}$$

$$- \frac{\tau - t_j}{t_j - t_{j-1}} A(t_{j-1}, S_{ph}, S_{cr}, X) \tag{37}$$

$$q_j(\tau, S_{ph}, S_{cr}, X) = \frac{\tau - t_{j-1}}{t_j - t_{j-1}} B(t_j, S_{ph}, S_{cr}, X) \tag{38}$$

$$- \frac{\tau - t_j}{t_j - t_{j-1}} B(t_{j-1}, S_{ph}, S_{cr}, X) \tag{39}$$

$$s_j(\tau, S_{ph}, S_{cr}, X) = \frac{\tau - t_{j-1}}{t_j - t_{j-1}} C(t_j, S_{ph}, S_{cr}, X) \tag{40}$$

$$- \frac{\tau - t_j}{t_j - t_{j-1}} C(t_{j-1}, S_{ph}, S_{cr}, X) \tag{41}$$

Then, we obtain

$$\begin{aligned} S_{ph}(t_{n+1}) - S_{ph}(0) &= \frac{1}{\Gamma(\alpha)} \sum_{j=0}^{n} \int_{t_j}^{t_{j+1}} p(\tau, S_{ph}, S_{cr}, X)(t_{n+1} - \tau)^{\alpha-1} d\tau \\ &= \sum_{j=0}^{n} \left[\frac{h^\alpha A(t_j, S_{ph}, S_{cr}, X)}{\Gamma(\alpha+2)} \left((n+1-j)^\alpha (n-j+2+\alpha) \right.\right. \\ &\left. -(n-j)^\alpha (n-j+2+2\alpha) \right)] \\ &- \sum_{j=0}^{n} \left[\frac{h^\alpha A(t_{j-1}, S_{ph}, S_{cr}, X)}{\Gamma(\alpha+2)} \left((n+1-j)^{\alpha+1} \right.\right. \\ &\left. -(n-j)^\alpha (n-j+1+\alpha) \right)] \end{aligned}$$

$$\begin{aligned} S_{cr}(t_{n+1}) - S_{cr}(0) &= \frac{1}{\Gamma(\alpha)} \sum_{j=0}^{n} \int_{t_j}^{t_{j+1}} q(\tau, S_{ph}, S_{cr}, X)(t_{n+1} - \tau)^{\alpha-1} d\tau \\ &= \sum_{j=0}^{n} \left[\frac{h^\alpha B(t_j, S_{ph}, S_{cr}, X)}{\Gamma(\alpha+2)} \left((n+1-j)^\alpha (n-j+2+\alpha) \right.\right. \\ &\left. -(n-j)^\alpha (n-j+2+2\alpha) \right)] \\ &- \sum_{j=0}^{n} \left[\frac{h^\alpha B(t_{j-1}, S_{ph}, S_{cr}, X)}{\Gamma(\alpha+2)} \left((n+1-j)^{\alpha+1} \right.\right. \\ &\left. -(n-j)^\alpha (n-j+1+\alpha) \right)] \end{aligned}$$

$$
\begin{aligned}
X(t_{n+1}) - X(0) &= \frac{1}{\Gamma(\alpha)} \sum_{j=0}^{n} \int_{t_j}^{t_{j+1}} s(\tau, S_{ph}, S_{cr}, X)(t_{n+1} - \tau)^{\alpha-1} d\tau \\
&= \sum_{j=0}^{n} \left[\frac{h^\alpha C(t_j, S_{ph}, S_{cr}, X)}{\Gamma(\alpha+2)} \left((n+1-j)^\alpha (n-j+2+\alpha)\right.\right. \\
&\left.\left. -(n-j)^\alpha (n-j+2+2\alpha)\right)\right] \\
&- \sum_{j=0}^{n} \left[\frac{h^\alpha C(t_{j-1}, S_{ph}, S_{cr}, X)}{\Gamma(\alpha+2)} \left((n+1-j)^{\alpha+1}\right.\right. \\
&\left.\left. -(n-j)^\alpha (n-j+1+\alpha)\right)\right]
\end{aligned}
$$

Thus, the computational scheme for the model with power law kernel has been obtained. We used this scheme and obtained Figures 1-4.

6 Analysis of the Model with the Exponential-decay Kernel

Next we analyze the model with FFD using the exponential-decay kernel as:

$$
{}_0^{FFE}D_t^{\alpha,\eta} S_{ph} = D\left(S_{ph0} - S_{ph}\right) - k_{ph} \cdot \mu\left(S_{ph}, S_{cr}\right) \cdot X, \tag{42}
$$

$$
{}_0^{FFE}D_t^{\alpha,\eta} S_{cr} = D\left(S_{cr0} - S_{cr}\right) - k_{cr} \cdot \mu\left(S_{ph}, S_{cr}\right) \cdot X, \tag{43}
$$

$$
{}_0^{FFE}D_t^{\alpha,\eta} X = -D\beta X + \mu\left(S_{ph}, S_{cr}\right) X \tag{44}
$$

The relationship between the fractal derivative and the classical derivative produces:

$$
{}_0^{CF}D_t^{\alpha} S_{ph} = \eta t^{\eta-1} \left(D\left(S_{ph0} - S_{ph}\right) - k_{ph} \cdot \mu\left(S_{ph}, S_{cr}\right) \cdot X\right), \tag{45}
$$

$$
{}_0^{CF}D_t^{\alpha} S_{cr} = \eta t^{\eta-1} \left(D\left(S_{cr0} - S_{cr}\right) - k_{cr} \cdot \mu\left(S_{ph}, S_{cr}\right) \cdot X\right), \tag{46}
$$

$$
{}_0^{CF}D_t^{\alpha} X = \eta t^{\eta-1} \left(-D\beta X + \mu\left(S_{ph}, S_{cr}\right) X\right) \tag{47}
$$

For simplicity, we define

$$
K(t, S_{ph}, S_{cr}, X) = \eta t^{\eta-1} \left(D\left(S_{ph0} - S_{ph}\right) - k_{ph} \cdot \mu\left(S_{ph}, S_{cr}\right) \cdot X\right), \tag{48}
$$

$$
L(t, S_{ph}, S_{cr}, X) = \eta t^{\eta-1} \left(D\left(S_{cr0} - S_{cr}\right) - k_{cr} \cdot \mu\left(S_{ph}, S_{cr}\right) \cdot X\right), \tag{49}
$$

$$
M(t, S_{ph}, S_{cr}, X) = \eta t^{\eta-1} \left(-D\beta X + \mu\left(S_{ph}, S_{cr}\right) X\right) \tag{50}
$$

Then, we obtain

$$
\begin{aligned}
{}_0^{CF}D_t^{\alpha} S_{ph} &= K(t, S_{ph}, S_{cr}, X) && (51)\\
{}_0^{CF}D_t^{\alpha} S_{cr} &= L(t, S_{ph}, S_{cr}, X) && (52)\\
{}_0^{CF}D_t^{\alpha} X &= M(t, S_{ph}, S_{cr}, X) && (53)
\end{aligned}
$$

Applying the CF integral yields [26]:

$$
\begin{aligned}
S_{ph}(t) - S_{ph}(0) =& \frac{1-\alpha}{M(\alpha)} K(t, S_{ph}, S_{cr}, X) \\
&+ \frac{\alpha}{M(\alpha)} \int_0^t K(\tau, S_{ph}, S_{cr}, X) d\tau \\
S_{cr}(t) - S_{cr}(0) =& \frac{1-\alpha}{M(\alpha)} L(t, S_{ph}, S_{cr}, X) \\
&+ \frac{\alpha}{M(\alpha)} \int_0^t L(\tau, S_{ph}, S_{cr}, X) d\tau \\
X(t) - X(0) =& \frac{1-\alpha}{M(\alpha)} M(t, S_{ph}, S_{cr}, X) \\
&+ \frac{\alpha}{M(\alpha)} \int_0^t M(\tau, S_{ph}, S_{cr}, X) d\tau
\end{aligned}
$$

Discretizing the above equations at t_{n+1} and t_n we get:

$$
\begin{aligned}
S_{ph}^{n+1} =& S_{ph}^0 + \frac{1-\alpha}{M(\alpha)} K(t_n, S_{ph}^n, S_{cr}^n, X^n) \\
&+ \frac{\alpha}{M(\alpha)} \int_0^{t_{n+1}} K(\tau, S_{ph}, S_{cr}, X) d\tau \\
S_{cr}^{n+1} =& S_{cr}^0 + \frac{1-\alpha}{M(\alpha)} L(t_n, S_{ph}^n, S_{cr}^n, X^n) \\
&+ \frac{\alpha}{M(\alpha)} \int_0^{t_{n+1}} L(\tau, S_{ph}, S_{cr}, X) d\tau \\
X^{n+1} =& X^0 + \frac{1-\alpha}{M(\alpha)} M(t_n, S_{ph}^n, S_{cr}^n, X^n) \\
&+ \frac{\alpha}{M(\alpha)} \int_0^{t_{n+1}} M(\tau, S_{ph}, S_{cr}, X) d\tau
\end{aligned}
$$

and

$$\begin{aligned}
S_{ph}^{n} =& S_{ph}^{0} + \frac{1-\alpha}{M(\alpha)} K(t_{n-1}, S_{ph}^{n-1}, S_{cr}^{n-1}, X^{n-1}) \\
&+ \frac{\alpha}{M(\alpha)} \int_{0}^{t_n} K(\tau, S_{ph}, S_{cr}, X) d\tau \\
S_{cr}^{n} =& S_{cr}^{0} + \frac{1-\alpha}{M(\alpha)} L(t_{n-1}, S_{ph}^{n-1}, S_{cr}^{n-1}, X^{n-1}) \\
&+ \frac{\alpha}{M(\alpha)} \int_{0}^{t_n} L(\tau, S_{ph}, S_{cr}, X) d\tau \\
X^{n} =& X^{0} + \frac{1-\alpha}{M(\alpha)} M(t_{n-1}, S_{ph}^{n-1}, S_{cr}^{n-1}, X^{n-1}) \\
&+ \frac{\alpha}{M(\alpha)} \int_{0}^{t_n} M(\tau, S_{ph}, S_{cr}, X) d\tau
\end{aligned}$$

Thus, we reach

$$\begin{aligned}
S_{ph}^{n+1} =& S_{ph}^{n} + \frac{1-\alpha}{M(\alpha)} \Big(K(t_n, S_{ph}^{n}, S_{cr}^{n}, X^{n}) - K(t_{n-1}, S_{ph}^{n-1}, S_{cr}^{n-1}, X^{n-1}) \Big) \\
&+ \frac{\alpha}{M(\alpha)} \int_{t_n}^{t_{n+1}} K(\tau, S_{ph}, S_{cr}, X) d\tau \\
S_{cr}^{n+1} =& S_{cr}^{n} + \frac{1-\alpha}{M(\alpha)} \Big(L(t_n, S_{ph}^{n}, S_{cr}^{n}, X^{n}) - L(t_{n-1}, S_{ph}^{n-1}, S_{cr}^{n-1}, X^{n-1}) \Big) \\
&+ \frac{\alpha}{M(\alpha)} \int_{t_n}^{t_{n+1}} L(\tau, S_{ph}, S_{cr}, X) d\tau \\
X^{n+1} =& X^{n} + \frac{1-\alpha}{M(\alpha)} \Big(M(t_n, S_{ph}^{n}, S_{cr}^{n}, X^{n}) - M(t_{n-1}, S_{ph}^{n-1}, S_{cr}^{n-1}, X^{n-1}) \Big) \\
&+ \frac{\alpha}{M(\alpha)} \int_{t_n}^{t_{n+1}} M(\tau, S_{ph}, S_{cr}, X) d\tau
\end{aligned}$$

Using the two-step Lagrange polynomial yields:

$$\begin{aligned}
S_{ph}^{n+1} =& S_{ph}^{n} + \frac{1-\alpha}{M(\alpha)}\left(K(t_n, S_{ph}^{n}, S_{cr}^{n}, X^{n}) - K(t_{n-1}, S_{ph}^{n-1}, S_{cr}^{n-1}, X^{n-1})\right) \\
&+ \frac{\alpha}{M(\alpha)}\left(\frac{3h}{2}K(t_n, S_{ph}^{n}, S_{cr}^{n}, X^{n}) - \frac{h}{2}K(t_{n-1}, S_{ph}^{n-1}, S_{cr}^{n-1}, X^{n-1})\right) \\
S_{cr}^{n+1} =& S_{cr}^{n} + \frac{1-\alpha}{M(\alpha)}\left(L(t_n, S_{ph}^{n}, S_{cr}^{n}, X^{n}) - L(t_{n-1}, S_{ph}^{n-1}, S_{cr}^{n-1}, X^{n-1})\right) \\
&+ \frac{\alpha}{M(\alpha)}\left(\frac{3h}{2}L(t_n, S_{ph}^{n}, S_{cr}^{n}, X^{n}) - \frac{h}{2}L(t_{n-1}, S_{ph}^{n-1}, S_{cr}^{n-1}, X^{n-1})\right) \\
X^{n+1} =& X^{n} + \frac{1-\alpha}{M(\alpha)}\left(M(t_n, S_{ph}^{n}, S_{cr}^{n}, X^{n}) - M(t_{n-1}, S_{ph}^{n-1}, S_{cr}^{n-1}, X^{n-1})\right) \\
&+ \frac{\alpha}{M(\alpha)}\left(\frac{3h}{2}M(t_n, S_{ph}^{n}, S_{cr}^{n}, X^{n}) - \frac{h}{2}M(t_{n-1}, S_{ph}^{n-1}, S_{cr}^{n-1}, X^{n-1})\right)
\end{aligned}$$

As a result, the model's computational scheme for the exponential decay kernel has been discovered. We used this scheme and obtained Figures 5-8.

7 Analysis of the Model with the Mittag-leffler Kernel

Now we analyze the model with FFD using the Mittag-Leffler kernel as:

$$\begin{aligned}
{}_{0}^{FFM}D_{t}^{\alpha,\eta}S_{ph} &= D\left(S_{ph0} - S_{ph}\right) - k_{ph}\cdot\mu\left(S_{ph}, S_{cr}\right)\cdot X, && (54)\\
{}_{0}^{FFM}D_{t}^{\alpha,\eta}S_{cr} &= D\left(S_{cr0} - S_{cr}\right) - k_{cr}\cdot\mu\left(S_{ph}, S_{cr}\right)\cdot X, && (55)\\
{}_{0}^{FFM}D_{t}^{\alpha,\eta}X &= -D\beta X + \mu\left(S_{ph}, S_{cr}\right)X && (56)
\end{aligned}$$

Then, we obtain

$$\begin{aligned}
{}_{0}^{AB}D_{t}^{\alpha}S_{ph} &= \eta t^{\eta-1}\left(D\left(S_{ph0} - S_{ph}\right) - k_{ph}\cdot\mu\left(S_{ph}, S_{cr}\right)\cdot X\right), && (57)\\
{}_{0}^{AB}D_{t}^{\alpha}S_{cr} &= \eta t^{\eta-1}\left(D\left(S_{cr0} - S_{cr}\right) - k_{cr}\cdot\mu\left(S_{ph}, S_{cr}\right)\cdot X\right), && (58)\\
{}_{0}^{AB}D_{t}^{\alpha}X &= \eta t^{\eta-1}\left(-D\beta X + \mu\left(S_{ph}, S_{cr}\right)X\right) && (59)
\end{aligned}$$

For simplicity, we define

$$Y(t, S_{ph}, S_{cr}, X) = \eta t^{\eta-1} \left(D \left(S_{ph0} - S_{ph} \right) - k_{ph} \cdot \mu \left(S_{ph}, S_{cr} \right) \cdot X \right), \quad (60)$$
$$Z(t, S_{ph}, S_{cr}, X) = \eta t^{\eta-1} \left(D \left(S_{cr0} - S_{cr} \right) - k_{cr} \cdot \mu \left(S_{ph}, S_{cr} \right) \cdot X \right), \quad (61)$$
$$T(t, S_{ph}, S_{cr}, X) = \eta t^{\eta-1} \left(-D\beta X + \mu \left(S_{ph}, S_{cr} \right) X \right) \quad (62)$$

Then, we get

$$ {}_0^{AB}D_t^{\alpha} S_{ph} = Y(t, S_{ph}, S_{cr}, X), \quad (63)$$
$$ {}_0^{AB}D_t^{\alpha} S_{cr} = Z(t, S_{ph}, S_{cr}, X), \quad (64)$$
$$ {}_0^{AB}D_t^{\alpha} X = T(t, S_{ph}, S_{cr}, X) \quad (65)$$

Applying the AB integral gives,

$$\begin{aligned}
S_{ph}(t) - S_{ph}(0) =& \frac{1-\alpha}{AB(\alpha)} Y(t, S_{ph}, S_{cr}, X) \\
&+ \frac{\alpha}{AB(\alpha)\Gamma(\alpha)} \int_0^t (t-p)^{\alpha-1} Y(p, S_{ph}, S_{cr}, X) dp, \\
S_{cr}(t) - S_{cr}(0) =& \frac{1-\alpha}{AB(\alpha)} Z(t, S_{ph}, S_{cr}, X) \\
&+ \frac{\alpha}{AB(\alpha)\Gamma(\alpha)} \int_0^t (t-p)^{\alpha-1} Z(p, S_{ph}, S_{cr}, X) dp, \\
X(t) - X(0) =& \frac{1-\alpha}{AB(\alpha)} T(t, S_{ph}, S_{cr}, X) \\
&+ \frac{\alpha}{AB(\alpha)\Gamma(\alpha)} \int_0^t (t-p)^{\alpha-1} T(p, S_{ph}, S_{cr}, X) dp.
\end{aligned}$$

Discretizing the above equations at t_{n+1}, we get:

$$\begin{aligned}
S_{ph}^{n+1} =& S_{ph}^{0} + \frac{1-\alpha}{AB(\alpha)} Y(t_{n+1}, S_{ph}^{n}, S_{cr}^{n}, X^{n}) \\
&+ \frac{\alpha}{AB(\alpha)\Gamma(\alpha)} \int_{0}^{t_{n+1}} (t_{n+1}-p)^{\alpha-1} Y(p, S_{ph}, S_{cr}, X)dp, \\
S_{cr}^{n+1} =& S_{cr}^{0} + \frac{1-\alpha}{AB(\alpha)} Z(t_{n+1}, S_{ph}^{n}, S_{cr}^{n}, X^{n}) \\
&+ \frac{\alpha}{AB(\alpha)\Gamma(\alpha)} \int_{0}^{t_{n+1}} (t_{n+1}-p)^{\alpha-1} Z(p, S_{ph}, S_{cr}, X)dp, \\
X^{n+1} =& X^{0} + \frac{1-\alpha}{AB(\alpha)} T(t_{n+1}, S_{ph}^{n}, S_{cr}^{n}, X^{n}) \\
&+ \frac{\alpha}{AB(\alpha)\Gamma(\alpha)} \int_{0}^{t_{n+1}} (t_{n+1}-p)^{\alpha-1} T(p, S_{ph}, S_{cr}, X)dp.
\end{aligned}$$

Then, we obtain

$$\begin{aligned}
S_{ph}^{n+1} =& S_{ph}^{0} + \frac{1-\alpha}{AB(\alpha)} Y(t_{n+1}, S_{ph}^{n}, S_{cr}^{n}, X^{n}) \\
&+ \frac{\alpha}{AB(\alpha)} \sum_{i=0}^{n} \left[\frac{h^{\alpha} Y(t_i, S_{ph}^{n}, S_{cr}^{n}, X^{n})}{\Gamma(\alpha+2)} \left((n+1-i)^{\alpha} (n-i+2+\alpha) \right.\right. \\
&\left.\left. -(n-i)^{\alpha}(n-i+2+2\alpha) \right) \right] \\
&- \frac{\alpha}{AB(\alpha)} \sum_{i=0}^{n} \left[\frac{h^{\alpha} Y(t_{i-1}, S_{ph}^{n-1}, S_{cr}^{n-1}, X^{n-1})}{\Gamma(\alpha+2)} \left((n+1-i)^{\alpha+1} \right.\right. \\
&\left.\left. -(n-i)^{\alpha}(n-i+1+\alpha) \right) \right]
\end{aligned}$$

$$\begin{aligned}
S_{cr}^{n+1} =& S_{cr}^{0} + \frac{1-\alpha}{AB(\alpha)} Z(t_{n+1}, S_{ph}^{n}, S_{cr}^{n}, X^{n}) \\
&+ \frac{\alpha}{AB(\alpha)} \sum_{i=0}^{n} \left[\frac{h^{\alpha} Z(t_i, S_{ph}^{n}, S_{cr}^{n}, X^{n})}{\Gamma(\alpha+2)} \left((n+1-i)^{\alpha} (n-i+2+\alpha) \right.\right. \\
&\left.\left. -(n-i)^{\alpha}(n-i+2+2\alpha) \right) \right] \\
&- \frac{\alpha}{AB(\alpha)} \sum_{i=0}^{n} \left[\frac{h^{\alpha} Z(t_{i-1}, S_{ph}^{n-1}, S_{cr}^{n-1}, X^{n-1})}{\Gamma(\alpha+2)} \left((n+1-i)^{\alpha+1} \right.\right. \\
&\left.\left. -(n-i)^{\alpha}(n-i+1+\alpha) \right) \right]
\end{aligned}$$

$$
\begin{aligned}
X^{n+1} =& X^0 + \frac{1-\alpha}{AB(\alpha)} T(t_{n+1}, S_{ph}^n, S_{cr}^n, X^n) \\
&+ \frac{\alpha}{AB(\alpha)} \sum_{i=0}^{n} \left[\frac{h^\alpha T(t_i, S_{ph}^n, S_{cr}^n, X^n)}{\Gamma(\alpha+2)} \left((n+1-i)^\alpha (n-i+2+\alpha) \right.\right. \\
&\left.\left. -(n-i)^\alpha (n-i+2+2\alpha) \right) \right] \\
&- \frac{\alpha}{AB(\alpha)} \sum_{i=0}^{n} \left[\frac{h^\alpha T(t_{i-1}, S_{ph}^{n-1}, S_{cr}^{n-1}, X^{n-1})}{\Gamma(\alpha+2)} \left((n+1-i)^{\alpha+1} \right.\right. \\
&\left.\left. -(n-i)^\alpha (n-i+1+\alpha) \right) \right].
\end{aligned}
$$

Thus, the computational scheme for the model with Mittag Leffler kernel has been obtained. We used this scheme and obtained Figures 9-12.

Remark 7.1. The distinctive advantage of utilizing Fractal-Fractional Derivatives (FFD) lies in its effectiveness to accurately characterize models for systems with memory effects. FFD enables the incorporation of operators with varying memories, aligning with the diverse relaxation processes observed in non-local dynamical systems. Consequently, models employing FFD prove to be notably advantageous and impactful in capturing the intricacies of these dynamic systems.

8 Results and Discussions

This section includes computational simulations for various fractional order and fractal dimension values. We discuss the results with the three different kernels as described in sections 5, 6 and 7. In these figure α, β and η are between zero and one. In these simulations, β is the parameter given on the model, η is fractal dimension and α is the fractional order. In Figure 1, we show the computational simulations for $\beta = 1$ and the fractal dimension $\eta = 1$ for different values of fractional order α with the power-law kernel. In this figure, we can see the impact of the fractional order α. In Figure 2, we show the computational simulations for $\beta = 1$ and the fractal dimension $\eta = 0.8$ for different values of fractional order α with the power-law kernel. In this figure, we can see the impact of the fractional order α. In Figure 3, we show the

computational simulations for $\beta = 0.5$ and the fractal dimension $\eta = 1.0$ for different values of fractional order α with the power-law kernel. In this figure, we can see the impact of the fractional order α. In Figure 4, we show the computational simulations for $\beta = 0.5$ and the fractal dimension $\eta = 0.9$ for different values of fractional order α with the power-law kernel. In this figure, we can see the impact of the fractional order α. In Figure 5, we show the computational simulations for $\beta = 1$ and the fractal dimension $\eta = 1$ for different values of fractional order α with the exponential-decay kernel. In this figure, we can see the impact of the fractional order α. In Figure 6, we show the computational simulations for $\beta = 1$ and the fractal dimension $\eta = 0.7$ for different values of fractional order α with the exponential-decay kernel. In this figure, we can see the impact of the fractional order α. In Figure 7, we show the computational simulations for $\beta = 0.8$ and the fractal dimension $\eta = 1$ for different values of fractional order α with the exponential-decay kernel. In this figure, we can see the impact of the fractional order α. In Figure 8, we show the computational simulations for $\beta = 0.8$ and the fractal dimension $\eta = 0.7$ for different values of fractional order α with the exponential-decay kernel. In this figure, we can see the impact of the fractional order α. In Figure 9, we show the computational simulations for $\beta = 1.0$ and the fractal dimension $\eta = 1.0$ for different values of fractional order α with the Mittag-Leffler kernel. In this figure, we can see the impact of the fractional order α. In Figure 10, we show the computational simulations for $\beta = 1.0$ and the fractal dimension $\eta = 0.5$ for different values of fractional order α with the Mittag-Leffler kernel. In this figure, we can see the impact of the fractional order α. In Figure 11, we show the computational simulations for $\beta = 0.5$ and the fractal dimension $\eta = 1.0$ for different values of fractional order α with the Mittag-Leffler kernel. In this figure, we can see the impact of the fractional order α. In Figure 12, we show the computational simulations for $\beta = 0.5$ and the fractal dimension $\eta = 0.6$ for different values of fractional order α with the Mittag-Leffler kernel. In this figure, we can see the impact of the fractional order α. In these figures, we can also see the impact of the parameter β and the impact of fractal dimension η.

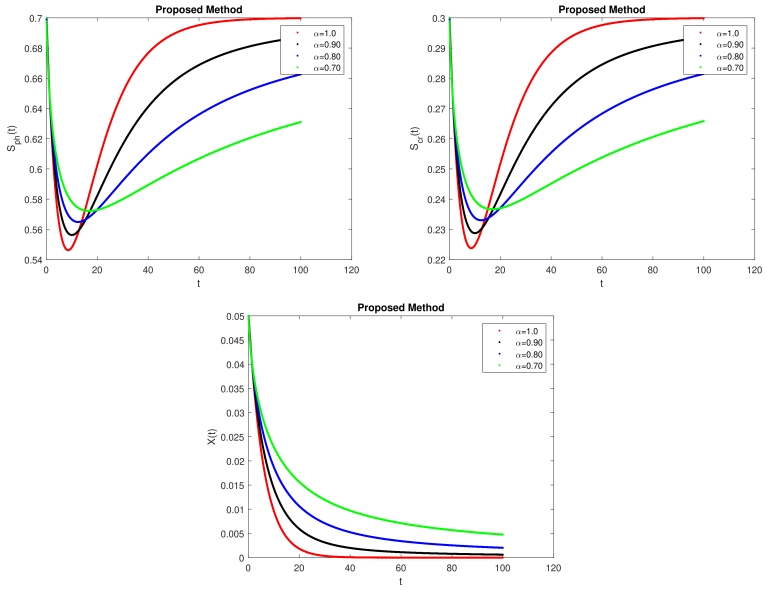

Figure 1: Computational simulations for $\beta = 1$ and the fractal dimension is 1 with the power-law kernel

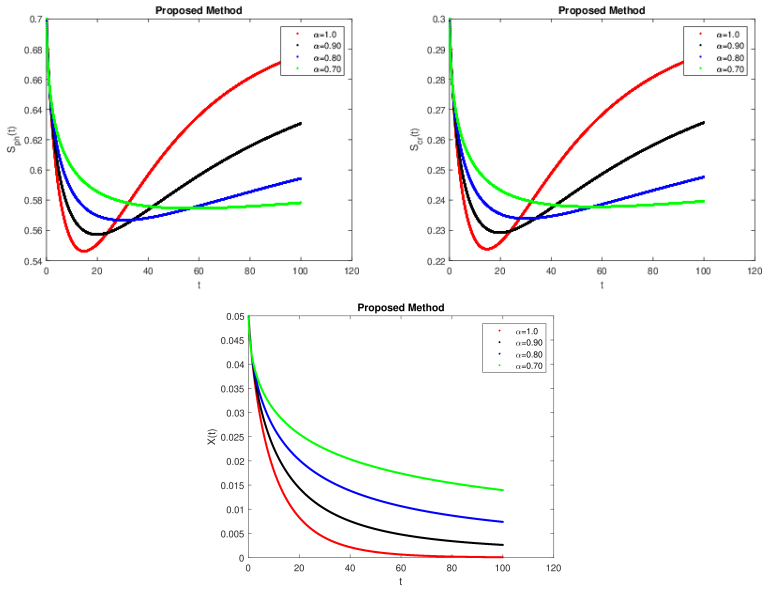

Figure 2: Computational simulations for $\beta = 1$ and the fractal dimension is 0.8 with the power-law kernel

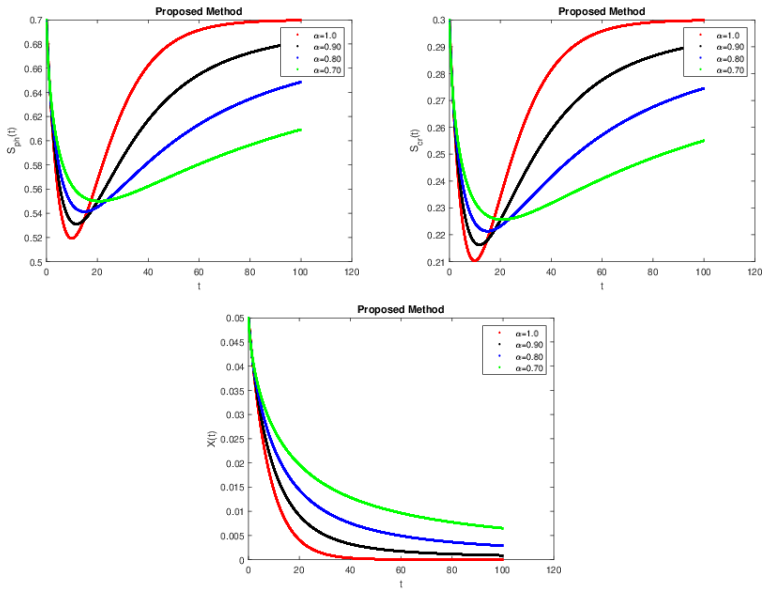

Figure 3: Computational simulations for $\beta = 0.5$ and the fractal dimension is 1 with the power-law kernel

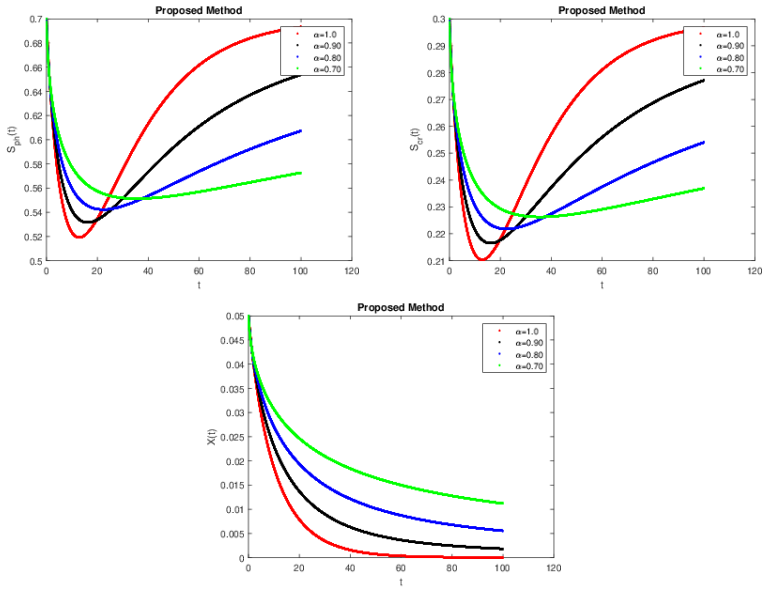

Figure 4: Computational simulations for $\beta = 0.5$ and the fractal dimension is 0.9 with the power-law kernel

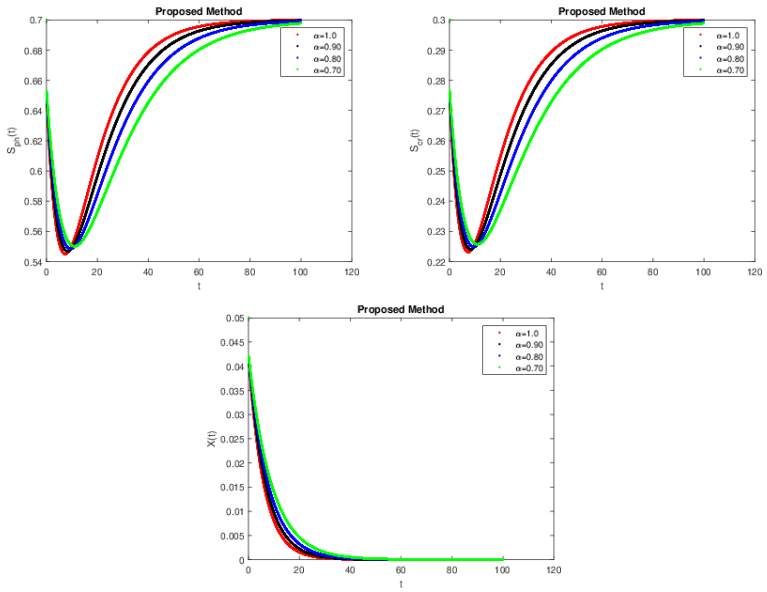

Figure 5: Computational simulations for $\beta = 1.0$ and the fractal dimension is 1 with the exponential-decay kernel

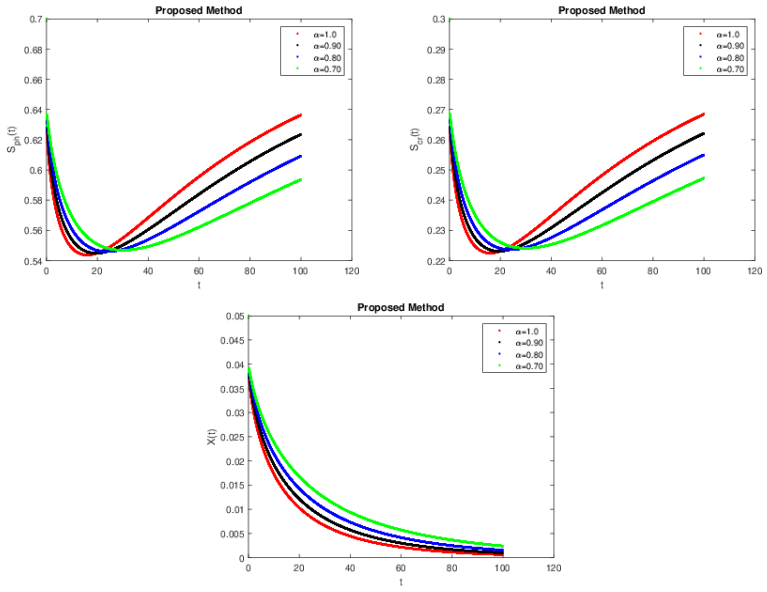

Figure 6: Computational simulations for $\beta = 1.0$ and the fractal dimension is 0.7 with the exponential-decay kernel

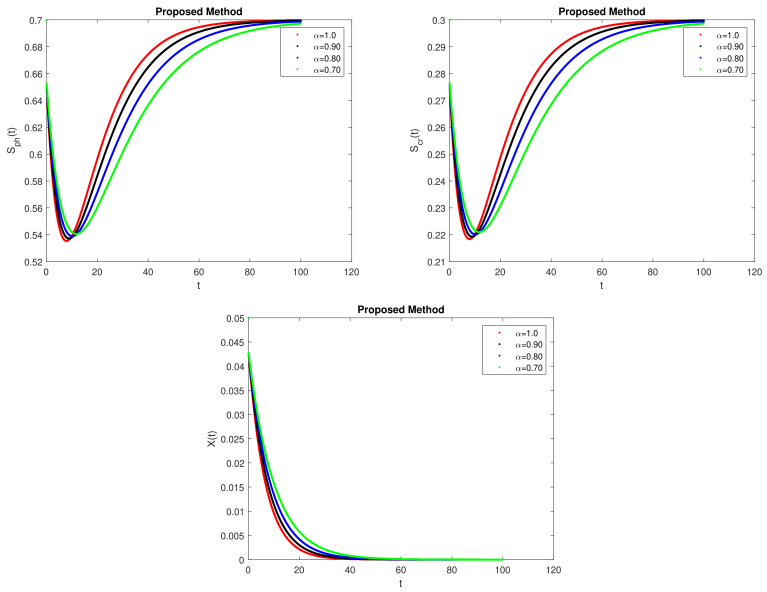

Figure 7: Computational simulations for $\beta = 0.8$ and the fractal dimension is 1.0 with the exponential-decay kernel

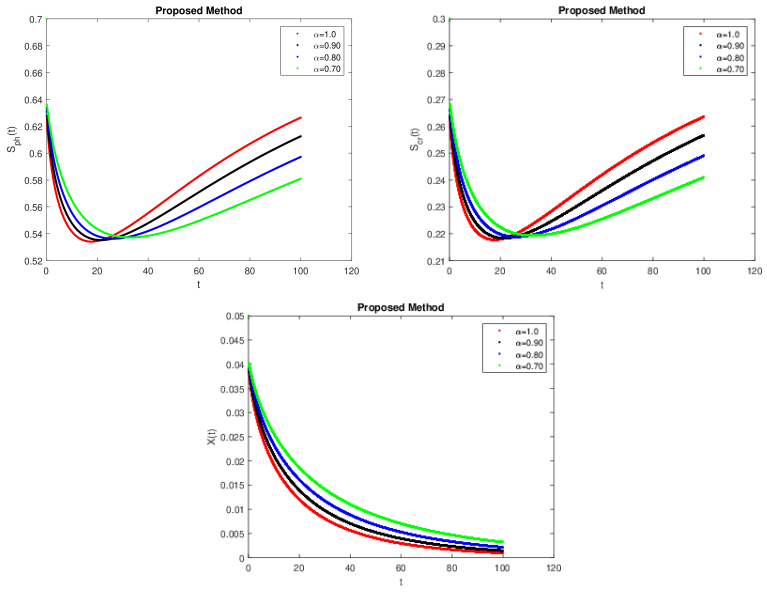

Figure 8: Computational simulations for $\beta = 0.8$ and the fractal dimension is 0.7 with the exponential-decay kernel

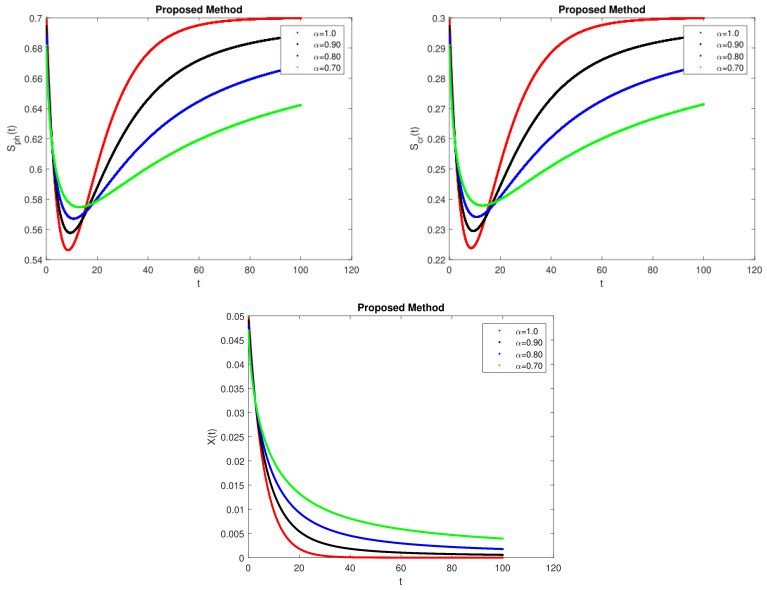

Figure 9: Computational simulations for $\beta = 1.0$ and the fractal dimension is 1.0 with the Mittag-Leffler kernel

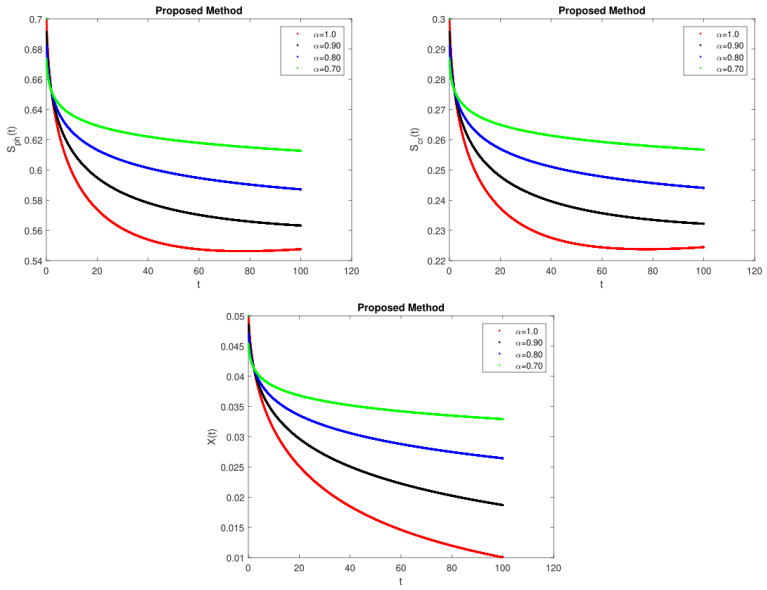

Figure 10: Computational simulations for $\beta = 1.0$ and the fractal dimension is 0.5 with the Mittag-Leffler kernel

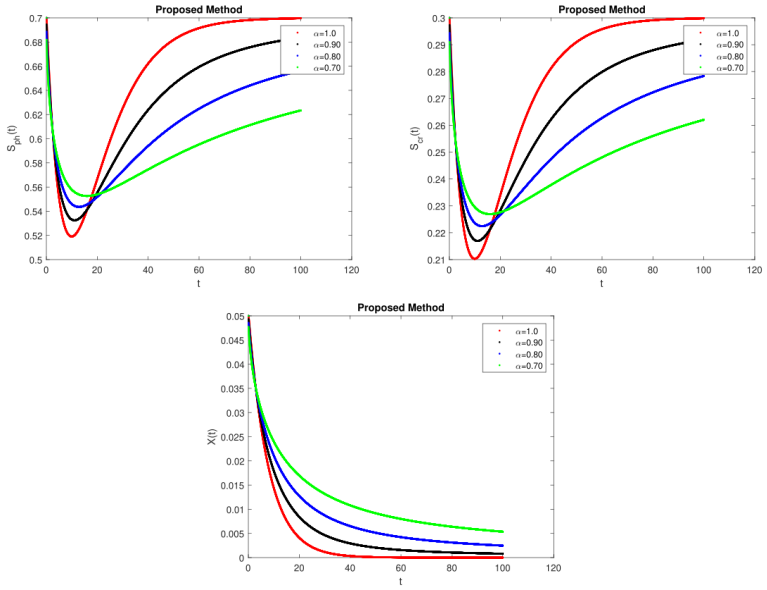

Figure 11: Computational simulations for $\beta = 0.5$ and the fractal dimension is 1.0 with the Mittag-Leffler kernel

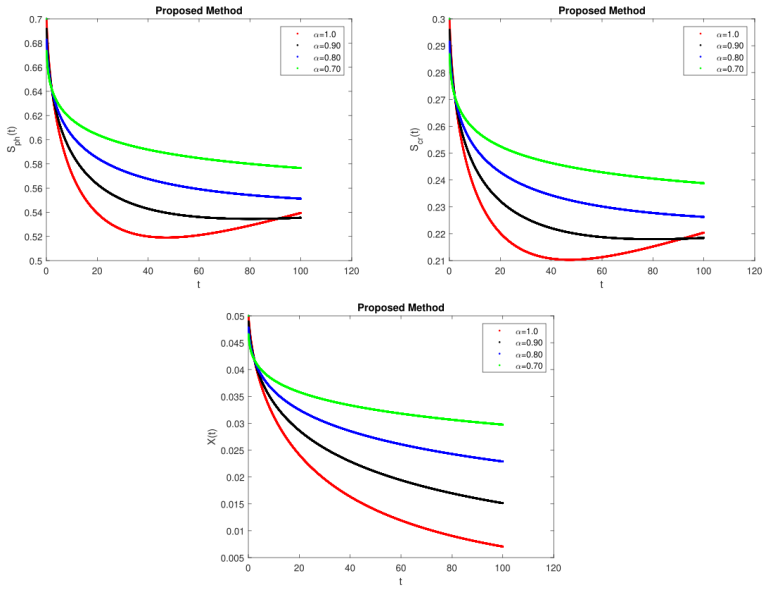

Figure 12: Computational simulations for $\beta = 0.5$ and the fractal dimension is 0.6 with the Mittag-Leffler kernel

9 Conclusion

In a continuously stirred bioreactor, a mathematical model for the breakdown of a phenol and p-cresol mixture was suggested in this manuscript. The model was based on three nonlinear ordinary differential equations. Analysis of their stability and determination of the model's equilibrium points were presented. Utilizing three alternative kernels, we also examined the model with the FFD and looked into the impacts of the fractional order and fractal dimension. For the concentrations of phenol, p-cresol, and biomass, we developed incredibly efficient computational approaches. To demonstrate the accuracy of the suggested technique, we gave the computational simulations for different values of α and β..

References

[1] Atangana A. , Fractal-fractional differentiation and integration: Connecting fractal calculus and fractional calculus to predict complex system, *Chaos, Solitons and Fractals* 102, (2017) 396–406.

[2] Alzabut J. , Selvam A. , Dhineshbabu R. , Tyagi S. , Ghaderi M. , Rezapour Sh. , A Caputo discrete fractional-order thermostat model with one and two sensors fractional boundary conditions depending on positive parameters by using the Lipschitz-type inequality, *Journal of Inequalities and Applications,* (2022), 1–24.

[3] Bhrawy A.H. , Doha E.H. , Ezz-Eldien S.S. and Van Gorder Robert A. , A new Jacobi spectral collocation method for solving $(1 + 1)$fractional Schrodinger equations and fractional coupled Schrodinger systems, *Eur. Phys. J. Plus* (2014), 129: 260.

[4] Boutiara, A., Alzabut, J., Ghaderi, M., and Rezapour, S., On a coupled system of fractional (p, q)-differential equation with Lipschitzian matrix in generalized metric space. *AIMS Mathematics*, 8(1), (2023), 1566-1591.

[5] Baleanu D. , Jajarmi A. , Mohammadi H. , Rezapour Sh. , A new study on the mathematical modelling of human liver with Caputo-

Fabrizio fractional derivative, *Chaos, Solitons and Fractals,* (2021), 134, 109705.

[6] Chen Y. , Yi M. , Chen C. , Yu C. , Bernstein Polynomials Method for Fractional Convection-Diffusion Equation with Variable Coefficients, *CMES*, vol.83, no.6, (2012), pp.639-653.

[7] Dimitrova N. , Zlateva P. , Global Stability Analysis of a Bioreactor Model for Phenol and Cresol Mixture Degradation. *Processes* (2021), 9, 124.

[8] El-Sayed A.M.A. , Gaber M. , The Adomian decomposition method for solving partial differential equations of fractal order in finite domains. *Phys. Lett. A.* 359, No 3 (2006), 175–182.

[9] Etemad S. , Avci I. , Kumar P. , Baleanu D. , Rezapour S. , Some novel mathematical analysis on the fractal-fractional model of the AH1N1/09 virus and its generalized Caputo-type version, *Chaos, Solitons and Fractals,* (2022), 162, 112511.

[10] George, R., Houas, M., Ghaderi, M., Rezapour, S., and Elagan, S. K., On a coupled system of pantograph problem with three sequential fractional derivatives by using positive contraction-type inequalities. *Results in Physics*, 39, (2022),105687.

[11] George, R., Aydogan, S. M., Sakar, F. M., Ghaderi, M., and Rezapour, S., A study on the existence of numerical and analytical solutions for fractional integrodifferential equations in Hilfer type with simulation. *AIMS Mathematics*, 8(5),(2023), 10665-10684.

[12] George, Reny, et al. On a coupled system of pantograph problem with three sequential fractional derivatives by using positive contraction-type inequalities. *Results in Physics* 39 (2022), 105687.

[13] George, R., Al-shammari, F., Ghaderi, M., and Rezapour, S., On the boundedness of the solution set for the ψ-Caputo fractional pantograph equation with a measure of non-compactness via simulation analysis. *AIMS Mathematics*, 8(9),(2023), 20125-20142.

[14] Huang F. , Liu F. , The fundamental solution of the space-time fractional advection-dispersion equation. *J. Appl. Math. Comput.* 18, No 1-2 (2005), 21-36.

[15] Heydarpour Z. , Izadi J. , George R. , Ghaderi M. , Rezapour Sh. , On a Partial Fractional Hybrid Version of Generalized Sturm–Liouville–Langevin Equation *Fractal and Fractional*, (2022), 6(5), 269.

[16] Karatay T., Bayramoglu S. R., Sahin A., Implicit difference approximation for the time fractional heat equation with the nonlocal condition, *Applied Computational Mathematics* 61 (2011) 1281–1288.

[17] Kietkwanboot A. , Chaiprapat S. , Müller R. , Suttinun O. , Biodegradation of phenolic compounds present in palm oil mill effluent as single and mixed substrates by Trameteshirsuta AK04. *J. Environ. Sci. Heal. Part A Toxic/Hazard. Subst. Environ. Eng.* (2020), 55, 989–1002.

[18] Li C. and Cao J. , A finite difference method for time-fractional telegraph equation, *IEEE/ASME International Conference on Mechatronics and Embedded Systems and Applications (MESA)*, (2012), 314–318.

[19] Liu F. , Anh V. , Turner I. , Computational solution of space fractional FokkerPlanck equation. *Journal of Computational and Applied Mathematics,* vol. 166, pp. (2004), 209 -219.

[20] Mohammadi, H., Kumar, S., Rezapour, S., and Etemad, S., A theoretical study of the Caputo–Fabrizio fractional modeling for hearing loss due to Mumps virus with optimal control. *Chaos, Solitons and Fractals*, 144,(2021), 110668.

[21] Matar, M. M., Abbas, M. I., Alzabut, J., Kaabar, M. K. A., Etemad, S., and Rezapour, S., Investigation of the p-Laplacian nonperiodic nonlinear boundary value problem via generalized Caputo fractional derivatives. *Advances in Difference Equations*, 2021(1),(2021), 1-18.

[22] Momani S. , An explicit and computational solutions of the fractional KdV equation. *Math. Comput. Simul.* 70, No 2 (2005), 110–118.

[23] Momani S. , Z. Odibat, Comparison between the homotopy perturbation method and the variational iteration method for linear fractional partial differential equations. *Comput. Math. Appl.* 54, No 7-8 (2007), 910–919.

[24] Seo, J. S., Keum, Y. S., and Li, Q. X.. Bacterial degradation of aromatic compounds. *International journal of environmental research and public health*, 6(1),(2009) 278-309.

[25] Sharma N. K. , Philip L. ,Bhallamudi S. M., Aerobic degradation of phenolics and aromatic hydrocarbons in presence of cyanide. *Bioresour. Technol.*(2012), 121, 263–273.

[26] Toufik M. , Atangana A. , New computational approximation of fractional derivative with non-local and non-singular kernel: application to chaotic models, *The European Physical Journal Plus* 132 (10), 444.

[27] Tomei M. C. , Annesini M. C , Biodegradation of phenolic mixtures in a sequencing batch reactor: A kinetic study. *Environ. Sci. Pollut. Res.* (2008), 15, 188–195.

[28] Yemendzhiev H. , Zlateva P. , Alexieva Z. , Comparison of the biodegradation capacity of two fungal strains toward a mixture of phenol and cresol by mathematical modeling. *Biotechnol. Biotechnol. Equip.*(2012), 26, 3278–3281.

Ali Akgül
Professor of Mathematics
Department of Mathematics,Siirt University, Siirt, Türkiye
Department of Electronics and Communication Engineering
Saveetha School of Engineering, Chennai, Tamilnadu, India
E-mail: aliakgul@siirt.edu.tr

Enver Ülgül
PhD of Mathematics
Department of Mathematics
Siirt University, Siirt, Türkiye
E-mail: enverulgul0244@hotmail.com

Rubayyi T. Alqahtani
Professor of Mathematics
Department of Mathematics and Statistics
Imam Mohammad Ibn Saud Islamic University, Riyadh, Saudi Arabia
E-mail: rtalqahtani@imamu.edu.sa